Journal of Thermal Analysis and Calorimetry, Vol. 56 (1999) 27–34

DTA-TG STUDY OF THE $CaO–SiO_2–H_2O$ AND $CaO–Al_2O_3–SiO_2–H_2O$ SYSTEMS UNDER HYDROTHERMAL CONDITIONS

D. S. Klimesch[1,2] *and A. Ray*[2]

[1]James Hardie & Coy Pty Limited, 1 Grand Avenue, Camellia, P.O. Box 219, Granville Sydney, NSW, 2142
[2]Materials Science, University of Technology, Sydney, P.O. Box 123, Broadway, Sydney NSW, 2007, Australia

Abstract

Simultaneous DTA-TG is an excellent technique for evaluating phases formed in hydrothermally treated $CaO–SiO_2–H_2O$ and $CaO–Al_2O_3–SiO_2–H_2O$ systems. Thermal analysis in combination with XRD and SEM, revealed that in the $CaO–Al_2O_3–SiO_2–H_2O$ system the amount of hydrogarnet formed was the largest when gibbsite was used as the Al source, smallest for kaolin and intermediate for metakaolin. The endotherm peak temperature of the hydrogarnet dehydration endotherm was affected by the amount of hydrogarnet and the Si content of hydrogarnet.

The thermal stability and structural order of 11 Å tobermorite were reduced with the incorporation of Al and, as a result, 11 Å tobermorite transformed into 9.3 Å tobermorite at lower temperatures while the transformation of the latter into beta-wollastonite required more energy. There exists a direct relationship between the 9.3 Å tobermorite and beta-wollastonite formation temperatures. Solid-state ^{29}Si and ^{27}Al MAS NMR data support these findings.

Keywords: Al-substituted 11 Å tobermorite, calcium silicate hydrate, derivative thermal curves, hydrogarnet, hydrothermal curing

Introduction

The evaluation of phase formations in the $CaO–Al_2O_3–SiO_2–H_2O$ system is of importance because of its relevance to cement and hydrothermally manufactured building products and insulating materials. In the presence of aluminium (Al) containing sources such as gibbsite, metakaolin or kaolin, the present authors have established, contrary to the general belief that Al-substituted 11 Å tobermorite precedes hydrogarnet, that it is in fact hydrogarnet which precedes Al-substituted 11 Å tobermorite and that hydrogarnet supplies most if not all of the Al to form the latter [1–4].

This paper illustrates how DTA-TG in combination with other techniques including XRD, solid-state ^{29}Si and ^{27}Al MAS NMR and SEM offer a powerful means for the evaluation of this rather complex system. The main focus of this paper is on hydrogarnet and Al-substituted 11 Å tobermorite formations.

1418–2874/99/ $ 5.00

Akadémiai Kiadó, Budapest
Kluwer Academic Publishers, Dordrecht

Experimental

The starting materials were mixtures of CaO, gibbsite, metakaolin (MK) or kaolin and either fine or coarse ground quartz. Details of raw material composition are given in Table 1. The starting composition with Ca/(Al+Si) bulk atom ratio of 0.8 and no added Al-source was 42.7% CaO and 57.3% quartz (fine or coarse). Seven additional mixtures prepared with gibbsite, MK (two types) or kaolin and either fine or coarse quartz had a bulk Ca/(Al+Si) atom ratio of 0.8 and contained approximately 6.4 % Al_2O_3; the resulting bulk Al/(Al+Si) atom ratio was 0.13 for all mixes. CaO was prepared by calcination of reagent-grade $CaCO_3$ (SIGMA, ACS reagent, assay 100.0%) at 1050°C for 5 h.

Table 1 Chemical composition of raw materials as determined by X-ray fluorescence (ignited basis)

Oxide	MK No. 1	MK No. 2	Kaolin	Gibbsite	Fine quartz	Coarse quartz
SiO_2	55.7	55.8	54.6	–	99.8	99.0
K_2O	2.17	0.37*	2.26	–	–	–
TiO_2	0.02	2.25	–	–	ND	ND
Al_2O_3	41.5	40.5	42.3	100	ND	ND
Fe_2O_3	0.51	0.64	0.59	–	ND	ND
P_2O_5	0.06	–	0.12	–	ND	ND
CaO	–	0.05	0.02	–	ND	ND

ND – not determined
*constitutes Na_2O+K_2O

Slurries were prepared by hydrating CaO in six parts of freshly-boiled deionised water at 50–60°C with stirring for 3 min. The amount of water required to give a water/total solids ratio of 4.5 was then added, followed by addition of previously weighed and homogenised quartz-Al-source mixtures. Stirring was continued for another 5 min. The resulting slurry was divided among 6 small Parr bombs (45 mL screw cap bomb fitted with needle valve) using a plastic syringe. These bombs were placed in a temperature-controlled oven, set at 100°C, and heated to 180°C in 40 min. They were removed from the oven after the following reaction times: 0 h (i.e. upon completion of the 40 min temperature ramp from 100 180°C) then 1, 2, 4, 9 and 23 h at 180°C. Each bomb was quenched in a bucket of water for 2 min, the steam released and the charge vacuum dried at 60°C for a minimum of 24 h. After vacuum drying, samples were manually ground for 4 min using a mortar and a pestle followed by an additional vacuum drying period. Slurry preparation, sample transfer and grinding were all conducted in a N_2-filled glove box to minimise the effects of atmospheric carbonation. Samples were examined as follows:

DTA-TG was carried out using a TA instrument SDT 2960 simultaneous DTA-TG analyser at a heating rate of 10°C min^{-1} under flowing nitrogen (100 mL min^{-1})

from 60–1050°C. Sample sizes were between 15–20 mg and were packed into a Pt-Rh crucible with 20 taps. All curves were evaluated using the TA Instruments' software. Two point rotations were carried out for all DT curves as described previously [5]. Mass losses were determined by employing both TG and DTG curves while peak temperatures were determined with the second derivative differential thermal curve as described by Klimesch and Ray [5, 6].

The diffraction profiles of powdered specimens, with and without 10 percent by mass of silicon powder (Goodfellow Metals, Cambridge, England) used as an internal standard for correction of the interplanar spacings, were recorded at Bragg angles between 2 and 80° 2 theta, using CuK_α radiation and employing a step size of 0.02° 2 theta and an 8 s count time per step (Siemens D-5000 diffractometer). The unit cell size of hydrogarnet was calculated using a least-squares refinement program. The Si content in hydrogarnet was estimated from the linear relationship between unit cell size and Si content as determined by Jappy and Glasser [7]. The (002) peak of 11 Å tobermorite was used for the calculation of crystallite size. Selected specimens were also heated to 300, 500, 800 and 950°C for 1.5 h in air followed by cooling in a desiccator and XRD examination.

Solid-state ^{27}Al and ^{29}Si MAS NMR of selected specimens were obtained using a Bruker DRX 300 MHz spectrometer. Solid-state ^{27}Al MAS NMR provided information on the Al coordination state while ^{29}Si MAS NMR data provided information on the silica connectivity. A more detailed account has been given elsewhere [3, 8].

Scanning electron microscopy (SEM) on carbon coated specimens was conducted at an accelerating voltage of 8 kV (Jeol 6300 SEM fitted with energy dispersive X-ray microanalysis system (EDS)).

Results and discussion

Hydrogarnet

In the present investigation, mass loss between 260–350°C has been ascribed to the main dehydration endotherm of hydrogarnet, a member of the series $C_3AS_{3-x}H_{2x}$, x=0 to 3. Figure 1 (a) depicts the relationships between endotherm peak temperatures and percent mass loss of hydrogarnet formed when using either gibbsite, metakaolin or kaolin as the Al-source and either fine or coarse quartz. The dashed lines with an arrow indicate the direction of reaction time, that is from 0 to 23 h of hydrothermal treatment. While this mass loss is subject to overlap due to the concurrent dehydration reactions of calcium silicate hydrates (C–S–Hs) in these temperature ranges [9], the data clearly show the following trends:

1. The effect of the Al-source on the amount of hydrogarnet formed decreased in the following order: gibbsite>metakaolin>kaolin.

2. The endotherm peak temperature tended to decrease with decreasing amount of hydrogarnet, that is with increasing reaction time.

3. The endotherm peak temperatures were generally higher when kaolin was used as the Al-source and comparable when either metakaolin of gibbsite were used. The

data for specimens prepared with gibbsite and either fine or coarse quartz, however, appeared more scattered suggesting the contribution of an additional factor on the endotherm peak temperatures other than that due to reduction in hydrogarnet amount.

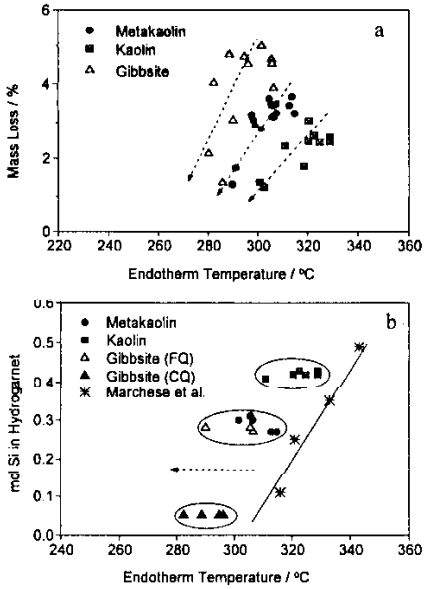

Fig. 1 Endotherm temperatures of the main dehydration endotherm of hydrogarnets *vs.* percent mass loss ascribed to hydrogarnets (a); endotherm temperatures *vs.* Si content (mol Si) in hydrogarnets. FQ – fine quartz, CQ – coarse quartz (b)

Yoder [10] found a dependence of the amount of energy required to drive out the OH groups on the percentage of Si present in hydrogarnet. The greater the percentage of Si present, the more tightly the hydroxyl groups are held and, as a consequence, the endotherm peak temperature increased. The relationship between endotherm peak temperatures and the Si content of hydrogarnet, as estimated from the unit cell size by XRD, manifested a similar trend (Fig. 1 (b)). Also included in this diagram is the data by Marchese *et al.* [11] for hydrothermally synthesized hydrogarnets with varying Si contents. The data (Fig. 1 (b)) explain the apparent anomaly between the endotherm peak temperatures and the percent mass loss of hydrogarnet formed for specimens prepared with gibbsite and either fine or coarse quartz as noted previously. Additionally, the data indicate the following:

1. Hydrogarnet composition did not change significantly with reaction time. It follows that the decrease in endotherm peak temperature with reaction time was a consequence of reduced hydrogarnet amount (Fig. 1 (a)).

2. The Si content of hydrogarnet was comparable when using either gibbsite and fine quartz or metakaolin and either fine or coarse quartz. It follows that metakaolin behaved as an (alumina+silica) source, presumably a consequence of its greater reactivity in comparison to the parent kaolin [12].

3. The Si content of hydrogarnet formed can be controlled by using gibbsite as the Al-source and 'adjusting' quartz reactivity.

4. The Si content of hydrogarnet was greatest when kaolin was the Al-source. Since hydrogarnet composition was unaffected when using either fine or coarse quartz, it follows that the reactivity of the alumino-silicate source, with kaolin being less reactive than its dehydroxylated counterpart metakaolin, also controls hydrogarnet composition.

From the previous discussion it is also clear that the endotherm peak temperature, due to the hydrogarnet dehydration reaction, is affected by both the amount of hydrogarnet present and its Si content. These findings may explain why some authors have not noted a relationship between the main endothermic peak temperature and the Si content in hydrogarnet [7]. Caution should thus be exercised when attempting to relate hydrogarnet composition with the endothermic peak temperature.

11 Å Tobermorite

As mentioned previously, the hydrogarnet precedes Al-substituted 11 Å tobermorite and supplies most if not all of the Al required for Al-substituted 11 Å tobermorite formation [1–4]. DTA, XRD and SEM provided clear evidence for these phenomena while solid-state ^{27}Al MAS NMR manifested a clear transformation in the Al coordination state from predominantly octahedral (hydrogarnet) to a combination of predominantly tetrahedral (Al-substituted 11 Å tobermorite) and some octahedral (hydrogarnet).

11 Å tobermorite possesses a layered structure with basal spacing of about 11 Å as determined by XRD [13]. Al^{3+} ions substitute for Si^{4+} ions in the four-fold or tetrahedrally coordinated sites [13]. The incorporation of Al into the structure causes a slight expansion in the basal spacing due to its larger ionic radius. Al-free and Al-substituted 11 Å tobermorites, are classed normal, mixed or anomalous depending on their thermal stability. For example, normal 11 Å tobermorites undergo a unidimensional lattice shrinkage by about 300°C to give approximately 9.3 Å tobermorite [13, 14]. The latter can be manifested by a mild exothermic deflection. The initial formation of the 9.3 Å hydrate at about 300°C may involve little or no interlayer condensation, water being lost predominantly from the molecules rather than Si OH groups [14, 15]. In contrast, anomalous 11 Å tobermorites retain their basal spacing upon dehydration [13, 14]. Ultimately, the 9.3 Å tobermorite continues to dehydrate and at about 800 to 830°C beta-wollastonite (β-CS) forms which is manifested by a mild exothermic deflection. Any excess silica, not required for β-CS formation, is expelled and is probably poorly crystalline [15].

Figure 2 (a) depicts the relationship between the main dehydration endotherm peak temperatures of 11 Å tobermorite and the exotherm peak temperatures due to the 9.3 Å tobermorite formation (where discernible) for both Al-free and Al-substituted 11 Å tobermorites. The following trends are clearly evident:

1. The thermal stability was lower for Al-substituted 11 Å tobermorites. The endotherms were generally broader for Al-substituted 11 Å tobermorites in comparison to the Al-free 11 Å tobermorites. This observation and the reduction in endotherm peak temperatures suggests a less ordered structure and that the water was less tightly held in the structure. Presence of structural disorder was confirmed, in particular, by solid-state ^{29}Si MAS NMR and was manifested by peak broadening and the presence of multiple shoulders in the spectra. A more detailed account has been given elsewhere [8].

2. The 9.3 Å tobermorite formation temperature was significantly lower for Al-substituted 11 Å tobermorites and signified normal thermal behaviour. In contrast Al-free tobermorites exhibited anomalous thermal behaviour. XRD examination of specimens heated for 1.5 h at 300°C confirmed unidimensional lattice shrinkage to approximately 9.3 Å tobermorite for all Al-substituted 11 Å tobermorites while Al-free tobermorites kept their basal spacing after dehydration. Possible explanations for these phenomena are as follows.

It is well known that hydrothermally prepared 11 Å tobermorites (Al-free and Al-substituted) contain double-chain silicate anion structures, that is numerous Si–O–Si bridges between two single chains forming double chains. Furthermore, the number of these Si–O–Si bridges affects the thermal stability of 11 Å tobermorites, that is the greater the number of these bridges the greater the thermal stability. Al is known to substitute into these bridging sites, forming Si–O–Al links, as well as into the silicate anion chains [13]. It follows that since the Al–O binding energy is lower than the Si–O binding energy, Al-containing bridging sites will be less stable. Furthermore, it has been shown that during thermal treatment a change occurs in the position of the Al-atoms in the 11 Å tobermorite structure [16]. The transfer of Al atoms, for example, may result in condensation reactions inside a single double-chain or between double-chains in one layer. Another possibility is that the Al-substituted 11 Å tobermorites contained fewer Si–O–Si bridges.

Figure 2 (b) illustrates the relationship between the exotherm peak temperatures due to the formation of β-CS and the exotherm peak temperatures due to the 9.3 Å tobermorite formation for both Al-free and Al-substituted 11 Å tobermorites. The presence of Al in the 11 Å tobermorite crystal lattice was manifested by XRD, solid-state ^{27}Al and ^{29}Si MAS NMR and by the increase in the exotherm temperature from about 830 to 840°C for Al-free 11 Å tobermorites to about 850 to 880°C. A more detailed account of the effects on the exotherm profile upon Al substitution has been given elsewhere [17].

XRD examination of specimens heated at 950°C for 1.5 h in air confirmed the presence of β-CS while this phase had not formed in specimens heated at 500°C and only partially in specimens heated at 800°C. This is in accordance with previous observations [15]. The data clearly show the following:

1. β-CS formation from Al-substituted 11 Å tobermorites required more energy than that from Al-free 11 Å tobermorites.

2. There exists a relationship between the 9.3 Å tobermorite formation temperature and the β-CS formation temperature.

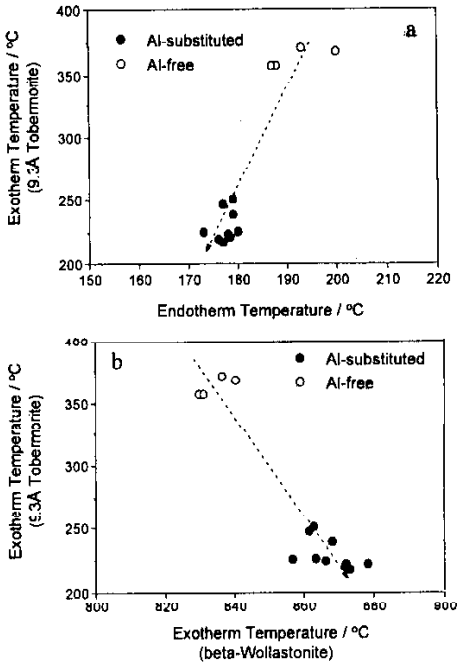

Fig. 2 Endotherm temperatures of the main dehydration endotherm of 11 Å tobermorites (Al-free and Al-substituted) *vs.* exotherm temperature due to 9.3 Å tobermorite formation and (a); exotherm temperature due to β-CS formation *vs.* exotherm temperature due to 9.3 Å tobermorite formation (b)

These observations can be rationalized as follows:

The conversion of 9.3 Å tobermorite into β-CS can be explained by the hypothesis of Si migration, with the Ca–O framework remaining almost unchanged, but the Si–O anions being partly destroyed and rebuilt [15]. For 11 Å tobermorites having a highly ordered silicate anion structure, such as the Al-free 11 Å tobermorites in this investigation, β-CS forms with comparative ease, since topotactic dehydration and crystallization reactions proceed at low energies [18]. It follows that, factors contributing to disorder of the silicate anion structures, such as Al incorporation into the 11 Å tobermorite crystal lattice, obstruct β-CS formation and as a consequence require chain ordering of the silicate anions and higher energies. This is corroborated by: the decrease in the endotherm peak temperature, the decrease in the exotherm peak temperature due to 9.3 Å tobermorite formation and the increase in the exotherm peak temperature due to the β-CS formation.

Conclusions

From the data presented in this paper we conclude the following:

1. The effect of the Al-source on the amount of hydrogarnet formed decreased in the following order: gibbsite>metakaolin>kaolin.

2. The endotherm peak temperature of the hydrogarnet dehydration endotherm is affected by the amount of hydrogarnet and the Si content of the hydrogarnet.

3. Hydrogarnet composition did not change significantly with reaction time.

4. The Si content of hydrogarnet formed decreased in the following order: kaolin> MK (fine or coarse quartz) ≈gibbsite (fine quartz)>>gibbsite (coarse quartz).

5. The incorporation of Al into the 11 Å tobermorite crystal lattice reduced its structural order and thermal stability and, as a consequence, Al-substituted 11 Å tobermorites exhibited normal thermal behaviour and transformed into 9.3 Å tobermorite at lower temperatures while the conversion of 9.3 Å tobermorite into β-CS required more energy.

References

1 D. S. Klimesch and A. Ray, Cem. Concr. Res., 28 (1998) 1109.
2 D. S. Klimesch and A. Ray, Cem. Concr. Res., (1998) (in press).
3 D. S. Klimesch and A. Ray, J. Amer. Ceram. Soc., (1998) (under review).
4 D. S. Klimesch and A. Ray, Thermochim. Acta, 316 (1998) 149.
5 D. S. Klimesch and A. Ray, Thermochim. Acta, 289 (1996) 41.
6 D. S. Klimesch and A. Ray, Thermochim. Acta, 307 (1997) 167.
7 T. G. Jappy and F.P. Glasser, Adv. Cem. Res., 4 (1991/92) 1.
8 D. S. Klimesch, A. Ray and G. Lee, (1998) (in preparation).
9 T. Mitsuda, S. Kobayakawa and H. Toraya, 8th Proc. Int. Congr. Chem. Cem., Vol. 3, 1986, p. 173.
10 H. S. Yoder, J. Geol., 58 (1950) 221.
11 B. Marchese, G. Mascolo and R. Sersale, J. Amer. Ceram. Soc., 55 (1972) 146.
12 D. S. Klimesch and A. Ray, J. Mater. Sci., (1998) (submitted for publication).
13 M. Tsuji, S. Komarneni and P. Malla, J. Amer. Ceram. Soc., 74 (1991) 274.
14 W. Wieker, A. R. Grimmer, A. Winkler, M. Mägi, M. Tarmak and E. Lippmaa, Cem. Concr. Res., 12 (1982) 333.
15 H. F. W. Taylor, 6th Natl. Conf. on Clays and Clay Minerals, 1959, p. 101.
16 R. Gabrovsek, B. Kurbus, D. Müller and W. Wieker, Cem. Concr. Res., 23 (1993) 321.
17 D. S. Klimesch and A. Ray, Thermochim. Acta, (1998) (under review).
18 K. Sasaki, T. Masuda, H. Ishida and T. Mitsuda, J. Amer. Ceram. Soc., 79 (1996) 1569.